Estimation of Spherical Refractive Errors Using Virtual Reality Headset

Ashish Goyal[1], Ajit Bopardikar[1] and Vijay Narayan Tiwari[1]

***Abstract*— Refractive errors are the most common visual defects in humans. They are corrected using lenses whose power is determined using expensive and bulky devices operated by trained professionals. This limits the outreach of eye-health care. We exploit commercial virtual reality (VR) setup to create a portable and inexpensive system for subjective estimation of spherical refractive errors. In doing so, we aim to keep hardware additions simple and to a minimum. We add a plain reflecting mirror in a VR headset to project optotypes on programmable focal planes at varying distances from the subject's eye. An interactive interface uses feedback from the user to estimate accommodation range and spherical refractive errors automatically. We compute the range and precision of our system, and validate them in a user trial study. The proposed setup strongly agrees with clinical subjective refraction.**

I. INTRODUCTION

Human eye is a complex imaging system, where objects at wide ranging distances are dynamically focused onto the retina. This is possible due to adjustable refractive power of the eye, originating from the combination of cornea and crystalline lens. While cornea provides a fixed refractive power, crystalline lens changes its shape to focus on objects at various distances. This adaptation of the lens shape is known as accommodation, and the range of distances where the eye can focus is called accommodation range.

Defects in the shape of the eyeball, cornea or the lens cause difficulty or inability to focus the light properly onto the retina. Such defects are called refractive errors and the symptoms may include blurred vision, double vision, headaches and eye-strain. Fig. 1 presents common types of refractive errors, their causes and consequences. Globally, more than two billion people have refractive errors [1] and 670 million live without corrective glasses, lenses or surgery, causing impaired vision [2]. In developing countries, on average only 20% of people with refractive errors have access to vision correction [3], [4], [5].

Methods for measuring refractive errors can be classified into two broad categories - *subjective* and *objective*. Objective methods detect and estimate refractive errors without actively involving the subject. In *Retinoscopy*, eye's fundus is illuminated and light reflex of the pupil is studied using a retinoscope. Most *autorefractors* including *Shack-Hartmann* technique [6] are based on Scheiner's principle [7]. These project known light patterns in the subject's eye and measure distortion of the images formed on the retina. Subjective methods require active participation of the subject. Refractive errors are measured by recording the subject's judgment on sharpness of the eye-chart after wearing various trial lenses. Existing systems for refraction assessment require specialized, bulky and expensive optical instruments, for e.g. retinoscopes, lasers and fundus cameras. Moreover, these require active involvement of a trained specialist. Portable systems to measure refractive error have been proposed including SVOne [8], OptiOpia [9] and NETRA [10]. However, these systems contain mechanically moving parts and complex optical instruments like electro-optical lens, laser, fundus camera and microlens arrays.

Advancement of mobile displays and virtual reality (VR) headsets has opened new avenues for remote eye-health care via interactive programs, minimizing dependency on trained specialists and cumbersome clinical setups. In this paper, we present a novel setup based on VR environment for estimation of refractive errors. We exploit geometrical optics to create a programmable depth perception by placing just a plain reflecting mirror inside a VR headset in front of a mobile screen display. The subject wears the VR headset normally as shown in Fig. 2 and interacts with a program through an input device (VR controller). Since we can control the depth at which objects are projected through software, we can determine focus range of the user's eyes and measure most common refractive errors - myopia, hyperopia and presbyopia. In this paper, we explain the design of our setup, display patterns and algorithms used for accurate and robust estimation of user's optical power and present the results of a user trial study to validate the setup.

II. DESIGN OF DEPTH PERCEPTION

We exploit geometrical optics to create a programmable depth perception. Optical setup of a typical VR environment is illustrated in Fig. 3. The display is held very close to the observer with a converging lens, creating a magnified and virtual image. Let us denote the focal length of the lens as f and its distance from the display as u_0. The virtual image is formed at a distance v_0 from the lens, given by the thin lens formula:

$$\frac{1}{v_0} = \frac{1}{u_0} - \frac{1}{f}, \quad f > 0, \quad u_0 < f \tag{1}$$

We introduce a tilted mirror between the display and the lens such that its reflecting side is facing the observer, as shown in Fig. 4. Let us assume that the mirror is tilted at an angle of θ radians from optical axis of the lens and this axis is normal to the display plane. It follows from the laws of reflection that the display and its reflected image subtend equal angles at the mirror, i.e. $\pi/2+\theta$. Therefore, acute angle between reflected image of the display and vertical axis is

[1]Ashish Goyal, Ajit Bopardikar and Vijay Narayan Tiwari are with Samsung Research Institute, Bangalore, Karnataka, India ag.goyal, ajit.b, vn.tiwari at samsung.com

978-1-5386-3646-6/18/$31.00 ©2018 IEEE

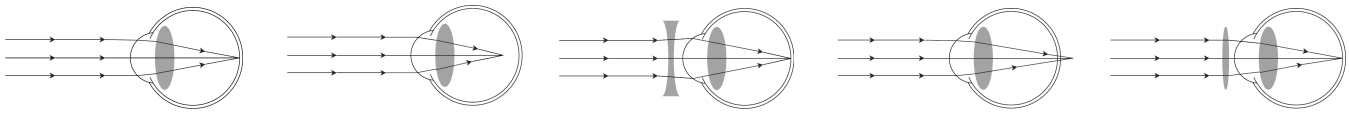

(a) (b) (c)

Fig. 1: Common refractive eye disorders and corrections. (a) Normal vision-rays from infinity focus on retina, (b) Myopia-rays converge before retina. Corrected using concave lens and (c) Hyperopia- rays converge behind retina. Corrected using covex lens.

Fig. 2: Users can estimate their spherical refractive errors by simply putting on the VR headset and interacting with the program using an input method like VR controller.

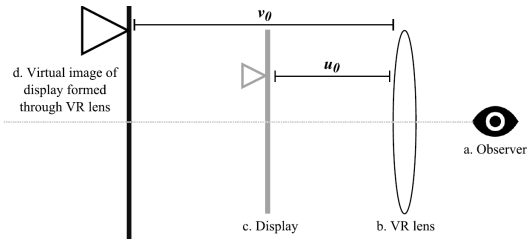

Fig. 3: Optical configuration of common VR setup. Display of the VR (c) is represented by the gray line and pointer and its virtual image (d) as seen by the observer (a) through the VR lens (b) is denoted by the black ones.

2θ as illustrated in Fig. 4. Consider a pixel on the display at a distance z from its center, as indicated by a marker in Fig. 4. Its reflection in the mirror, as depicted by the gray dashed marker, is at a distance $v_1 = u_0 + z\ sin(2\theta)$ from the lens along its optical axis. When seen through the lens, virtual image of this reflection is formed at a distance $v2$ given by:

$$\frac{1}{v_2} = \frac{1}{v_1} - \frac{1}{f} = \frac{1}{u_0 + z\ sin(2\theta)} - \frac{1}{f} \tag{2}$$

Thus using just a plane reflecting mirror, we achieve projection of displayed objects at programmable distances from the observer by changing display pixel coordinates.

A. System Calibration

Eq. 2 relates depth of a pixel perceived by the observer (v_2) to the pixel's coordinates on the display (z) and system's parameters - focal length of the lens (f), distance of the display from the lens (u_0) and inclination angle of the mirror (θ).

Notice that f can be obtained from VR headset manufacturer's specifications and θ can be chosen while designing the mirror add-on. Moreover, z is the product of pixel pitch (inverse of pixel density) and pixel coordinates. However, f and θ are subject to manufacturing imprecisions and u_0 is generally adjustable. Therefore, it is important to verify the system parameters by optically calibrating the setup.

We displayed grid like patterns at different values of z and found the projected distance of the pattern by manually focusing on it using a SLR camera kept near the VR headset. We used Samsung Gear VR and Galaxy S8 in our experiments. Specified focal length (f) for the Gear VR is 50mm

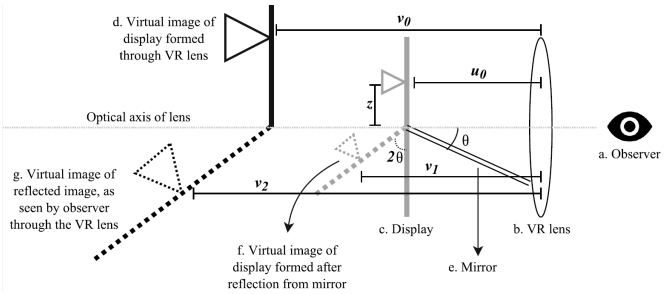

Fig. 4: Optical configuration of our setup after modifications to the VR environment. Reflected image of the display is depicted by the gray dashed line and pointer (f). Virtual image of this reflected image is seen by the observer through the lens, represented by black dashed line and pointer (g).

(20 D) and pixel-pitch of Galaxy S8 display is $4.46 \times 10^{-5} m$. We inclined the mirror at $\theta = 15°$ from optical axis of the lens to ensure minimum blocking of screen's reflection due to VR headset's lens case. We fixed our display at the closest possible distance from the lens (34cm) to maximize the range of $1/v_2$. Using these values in Eq. 2, we obtain inverse of projected distance as a function of displayed object's vertical coordinate in pixels. Data obtained during calibration process agrees with this function, as evident from Fig. 5.

B. Precision and Range

Eq. (2) can be used to find the nearest and furthest of distances at which our system can project, along with precision of depth control. To find the range of our system, we find minimum and maximum of $1/v_2$ in Eq. 2 subject to constraints of system parameters. Using the values obtained in Section II-A:

$$\frac{1}{v_2} = \frac{1}{0.034 + 4.46 \times 10^{-5} y\ sin(30°)} - \frac{1}{0.050} \tag{3}$$

where $y = z/\mu$ is vertical coordinate of the displayed object in pixels and μ is the pixel pitch. We used Galaxy S8 with the screen resolution of 2960×1440. Due to the mirror placed in front of the display, only half of the total screen is usable. Thus the range of y is $(0, 720)$ pixels and consequently, the range of $1/v_2$ is $(-4.8, 9.4)\ m^{-1}$. Theoretically, our setup can measure spherical corrective power from -9.4 to

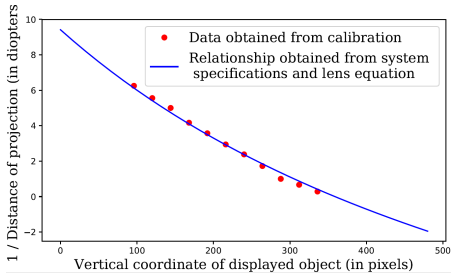

Fig. 5: Calibration data verifies the relationship between projected distance of displayed object and its vertical coordinate on the display (Eq. 2).

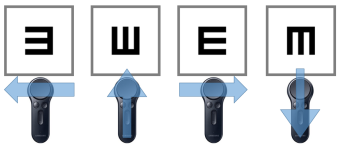

Fig. 6: Optotypes displayed in the tumbling E chart and corresponding expected response. Arrows superimposed on the Gear VR controller depict the swipe direction for a particular optotype.

+4.8 diopters (D). However, this theoretical range cannot be utilized completely due to the thickness of reflecting mirror and the limits of field of view of the VR headset. Precision $\Delta(1/v_2)$ in diopters can be calculated by:

$$\begin{aligned}\Delta\left(\frac{1}{v_2}\right) &= \left|\frac{\partial v_2}{\partial y}\right| \cdot \Delta y \\ &\leq max\left\{\left|\frac{-\mu sin(2\theta)}{(u_0+\mu y\, sin(2\theta))^2}\right|\right\} \cdot \Delta y \\ &\leq \left|\frac{\mu sin(2\theta)}{u_0^2}\right| \cdot \Delta y\end{aligned} \tag{4}$$

Note that in above equation $(u_0+\mu y\, sin(2\theta))^2$ is minimum when $y = 0 \;\; \forall \;\; \theta \in (0, \pi/2)$. Here Δy is the minimum possible change in pixel coordinate, trivially 1. Therefore, precision of inverse of depth projection is 1.93×10^{-4} D, well below clinical significance (0.25 D).

III. Estimating Accommodation Range

As shown in Eq. 2, perceived depth of a pixel can be controlled precisely by varying its coordinates on the display. By exploiting this phenomenon, we simulate the trial lens and eye-chart setup inside the VR headset. We display different symbols (optotypes) at controlled depths and record subject's feedback on perceived clarity of these optotypes using a Gear VR controller. Registering subject's feedback on conventional charts like Snellen or logMAR [11] using a typical VR controller is difficult owing to limited number of controls offered by these input methods. Therefore, we propose adaptation of a standard eye chart.

A. Display Patterns - Optotypes

Letter "E" of *Tumbling E chart* [12] oriented randomly in one of the four directions - *right*, *up*, *down* and *left* is displayed and the subject is asked to swipe on VR controller in corresponding direction (see Fig. 6). Subject can double tap on the controller if the displayed optotype appears blurred and he/she is unable to identify its orientation.

It is noteworthy that although magnification factor of every pixel depends upon its vertical coordinate, humans can only perceive the angle subtended by an its image on their eyes. Since image magnification increases linearly with its distance from the lens, angle subtended by the pixel's image remains approximately the same (VR lens to eye separation is small enough to be ignored). Therefore, independent of its location and consequently the projected depth, every pixel appears to be of approximately the same size.

As evident from Fig. 4, due to reflection from the inclined mirror, the final image as seen by observer is tilted. A finite sized object's vertical angle subtended on the observer's eye shrinks by a factor of $cos(2\theta)$, creating a distortion. We elongate the displayed objects by a factor of $1/cos(2\theta)$ along their vertical dimension to overcome this distortion.

B. Estimating Accommodation Range

We assess each eye independently and while one of the eye is being tested, the other eye's view is completely blacked out. We display optotypes using the scheme described in Section III-A, at projected distances from D_{min} to ∞, where D_{min} is the minimum possible projection distance of our setup (see Section II-A). We record multiple observations at every distance to make system robust to guessing. We increase the projected distance in a way such that its inverse decreases in steps of $\Delta P = 0.25$D, pegging system's precision for accommodation range estimation to be 0.25D.

For each observation, three types of subject feedback are possible - correct, incorrect and uncertain response (see Section III-A). When a subject registers multiple incorrect and/or uncertain response for a particular distance, we infer that he/she cannot accommodate to that distance. Starting from D_{min}, i.e. the minimum distance at which our setup can project, we gradually move the projection further and find the nearest distance at which the subject registers all correct responses and denote it as his/her near point. Similarly, starting from ∞, we gradually move the projection closer and find the furthest distance at which all of the subject's responses are correct and mark it as his/her far point.

C. Suggestive Refractive Error Correction

Finding corrective prescription of subject's eye is an involved procedure, where an eye doctor analyzes results of objective and subjective refraction and uses his judgment to arrive at prescription [13]. Our setup can be used to provide indicative optical power correction for near and far vision. Although we validated our setup only on myopic subjects, it can be easily extended to test hyperopia and presbyopia using following procedure:

Myopia: Optical power of the lens required to correct blurry far vision can be inferred directly from the subject's far point. Assuming the far point is d_{far}, it follows from the lens equation that the corrective power needed to help the subject focus at optical infinity is $P_{far} = -1/d_{far}$.

Hyperopia: An equivalent of "push plus" [13] can be performed. Start from $v_2 = D_{max}$, the furthest distance beyond infinity at which our system can project (in Eq. (2), $v_1 > f$, $v_2 < 0$), and gradually move the projection plane towards infinity until the subject registers all correct responses at some distance, say d_{hyp}. The plus spherical corrective power can be calculated as $P_{hyp} = -1/d_{hyp}$ ($d_{hyp} < 0$, beyond infinity).

Presbyopia: When both near and far vision become blurred, separate spherical correction power is required for each. Far vision exactly as in the case of myopia. Near vision is corrected using positive spherical power which can be inferred from near point of the subject (Section III-B), say d_{near}. If the ideal near point is d_{ideal} (it is subjective and depends on ideal reading distance of every

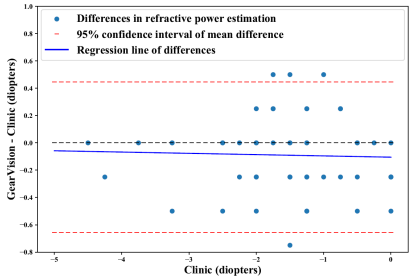

Fig. 7: Bald and Altman difference plot for spherical refractive power between GearVision and Clinic.

subject [13]), required plus power is calculated as $P_{near} = 1/d_{ideal} - 1/d_{near},\ \forall\, d_{near} > d_{ideal}$.

IV. User Trial Study

50 eyes - either healthy or myopic, were analyzed in our trial study, after ignoring subjects having astigmatism or with refractive power outside the range of our setup (see Table I for summary statistics). Participants ranged in age from 22 to 65 (mean $\pm$ standard deviation (SD): 28 ± 11 years). Each participant was tested for myopia with proposed setup (GearVision) and the results were compared with standard subjective refraction performed in clinic (Clinic). For all experiments, prior consent was taken from subjects, the data was kept anonymized and was used only for the intended research purpose. Additionally, principles outlined in the Helsinki Declaration were adhered to.

TABLE I: Summary of spherical power for GearVision and Clinic (50 eyes).

Summary Statistic	Clinic (D)	GearVision (D)
Mean	-1.83	-1.85
SD	1.11	1.11
Range	[-4.5, 0]	[-4.5, 0]

A. Accuracy

Table II summarizes comparison of GearVision with clinical subjective refraction. Small myopic bias of -0.03 is observed when GearVision is compared to clinical refraction. Mean of absolute differences is less than 0.25D, often considered as precision of prescription in optometric practice. Moreover, 78% of estimated refractive errors agreed within $\pm 0.25D$ with clinical test and 98% within $\pm 0.50D$. Although limits of agreement (95% LoA) in differences of GearVision and clinical refraction are around $(-0.65, 0.45)$D, it must be noted that subjective refraction is inherently variable [14]. Influence of pupil size during multiple tests of the same subject should also be accounted for while interpreting the results.

B. Reproducibility

12 participants and 24 eyes - either healthy or myopic, were tested on consecutive days using GearVision. Subjects with astigmatism or having refractive power outside the range of our setup were ignored. Age varied from 22 to 46 years (mean $\pm$ SD : 26.8 $\pm$ 7.8 years) with a manifest spherical power between -3.75 D to 0.00 D (mean $\pm$ SD : -1.77 $\pm$ 1.17 D). 95.8% of measurements have absolute differences less than or equal to 0.25D and 100% of them less than or equal to 0.50D. A summary of observations

TABLE II: Comparison between measurements from GearVision and Clinic. Error (Δ) : GearVision - Clinic.

Statistic Name	Value	Statistic Name	Value
Mean Δ (D)	-0.03	Maximum Δ (D)	0.50
Mean absolute Δ (D)	0.22	$\lvert\Delta\rvert \leq$ 0.25D (%)	78
SD of Δ (D)	0.28	$\lvert\Delta\rvert \leq$ 0.50D (%)	98
Minimum Δ (D)	-0.75		

TABLE III: Intra-subject precision statistics for differences (Δ) in estimated refractive power on two consecutive days using GearVision.

Statistic Name	Value	Statistic Name	Value
Mean Δ (D)	0.01	Maximum Δ (D)	0.50
Mean absolute Δ (D)	0.20	$\lvert\Delta\rvert \leq$ 0.250D (%)	95.8
SD Δ (D)	0.24	$\lvert\Delta\rvert \leq$ 0.125D (%)	62.5
Minimum Δ (D)	-0.50		

in Table III suggests low intra-subject variability and high reproducibility.

V. Conclusions

In this paper, we presented a VR based system for refractive error assessment. Our aim was to use commercial VR systems with minimal hardware modifications. We designed a mirror based add-on for depth simulation enabling us to perform subjective refraction. Experiments suggest that the proposed method is in good agreement with gold standard and produces reproducible results under clinical significance (0.25D). The proposed system currently measures spherical refractive errors. In future, we intend to extend the system to include astigmatism as well.

References

[1] Pradhan K. Thulasiraj RD, Aravind S. Spectacles for the millions addressing a priority of "vision 2020 - the right to sight". *Community Ophthalmology*, 3:19–21, 2003.

[2] Kempen JH et al. The prevalence of refractive errors among adults in the united states, western europe and australia. *Arch Ophthalmol.*, 122:495–505, 2004.

[3] Kovin S. Naidoo et al. Refractive error and visual impairment in african children in south africa. *Investigative Ophthalmology & Visual Science*, 44(9):3764, 2003.

[4] Shaheen P. Shah et al. Refractive errors in the adult pakistani population: The national blindness and visual impairment survey. *Ophthalmic Epidemiology*, 15(3):183–190, 2008.

[5] Rupert R. A. Bourne et al. Correction of refractive error in the adult population of bangladesh: Meeting the unmet need. *Investigative Ophthalmology & Visual Science*, 45(2):410, 2004.

[6] Ben C. Platt; Roland Shack. History and principles of shack-hartmann wavefront sensing. *Journal of Refractive Surgery*, 17, 2001.

[7] By CLARENCE W. MORRIS. The scheiner optometer. *The Australian Journal of Optometry*, 49(11):321–329, 1966.

[8] Smart Vision Labs. https://www.smartvisionlabs.com/autorefractors/.

[9] David Grosof. http://www.optiopia.com/.

[10] Vitor F. Pamplona et al. Netra: interactive display for estimating refractive errors and focal range. *ACM Trans. Graph.*, 29:77:1–77:8, 2010. Proceedings of SIGGRAPH 2010.

[11] Frederick L. Ferris III et al. New visual acuity charts for clinical research. *American Journal of Ophthalmology*, 94:91–96, 07 1982.

[12] R A Bourne et al. Evaluating a new logmar chart designed to improve visual acuity assessment in population-based surveys. *Eye*, 17, 2003.

[13] R.J. Kolker and L.D. Anderson. *Subjective Refraction and Prescribing Glasses: The Number One (or Number Two) Guide to Practical Techniques and Principles*. Joint Commission of Allied Health Personnel In Ophthalmology, 2015.

[14] G. Cleary et al. Diagnostic accuracy and variability of autorefraction by the tracey visual function analyzer and the shin-nippon nvision-k 5001 in relation to subjective refraction. *Ophthalmic and Physiological Optics*, 29(2):173–181, 2009.